Food & Function

ROYAL SOCIETY OF CHEMISTRY

PAPER

View Article Online
View Journal

Cite this: DOI: 10.1039/d3fo05704f

The dairy-derived peptide Miltin exerts anti-obesity effects by increasing adipocyte thermogenesis†

Hong Zhong,‡ Xiaoxiao Zhang,‡ Yangyang Wu, Lu Li, Zhuo Zhang, Xia Chi,* Xianwei Cui * and Chenbo Ji *

Received 9th January 2024,
Accepted 10th April 2024

DOI: 10.1039/d3fo05704f

rsc.li/food-function

Growing research has highlighted that the consumption of dairy products improves the metabolic health in obese individuals by functioning as regulatory modulators. However, the molecular basis of this effect remains largely unknown. Herein, we report a dairy-derived peptide, which we named Miltin, that activates the thermogenesis of brown adipocytes and increases white adipocyte browning. Previously, Miltin was merely identified for its antioxidant capacity, although it is commonly present in different dairy products. In this study, we revealed the effect of Miltin in modulating adipose thermogenesis and further explored its potential in treating obesity through *in vivo* and *in vitro* strategies. The administration of Miltin in mice fed with a high-fat diet resulted in enhanced thermogenesis, improved glucose homeostasis, and reduced body mass and lipid accumulation, indicating the anti-obesity effect of Miltin. Genomic analysis revealed that Miltin modulates thermogenesis by inducing the activation of the MAPK signaling pathway by preferentially interacting with GADD45γ to promote its stability. Together, our findings indicate that Miltin's role in initiating the thermogenesis of adipocytes makes it a potential anti-obesity therapy for future development.

1. Introduction

The prevalence of obesity and its associated comorbidities, including type 2 diabetes (T2D) and cardiovascular diseases, makes obesity a major healthcare challenge worldwide.[1] More effective and accessible therapies are urgently needed because lifestyle and behavioral interventions have proven mostly ineffective.[2] The underlying cause of obesity is an imbalance between energy intake and expenditure.[2] Thus, manipulating energy expenditure in the adipose tissue can potentially be an effective therapeutic measure for obesity and, consequently, for metabolic disease treatment. There are two types of thermogenic fat cells: classical brown adipocytes, which reside in brown adipose tissues (BATs) and beige adipocytes, which emerge from white adipose tissues (WATs).[3,4] These cells could contribute to energy dissipation *via* uncoupling protein 1 (UCP1)-mediated non-shivering thermogenesis.[3,4] Thus, promoting BAT activation or WAT browning becomes an attractive approach to combat obesity.[5–7]

Although controversial, it has been proposed that dairy product consumption supplies beneficial effects on obesity and metabolic syndrome.[8,9] A meta-analysis, based on cohort studies, elucidated the relative risks between the consumption of different dairy subtypes and obesity and reported that a higher intake of total dairy, milk, and yogurt is inversely associated with overweight or obesity.[10] Moreover, a recent study demonstrated that yogurt consumption improved glucose homeostasis and insulin sensitivity in obese mice.[11] Analytically, milk fermentation-derived branched chain hydroxy acids were identified as metabolic regulators that improved glucose metabolism in both hepatocytes and myocytes *via* a cell-autonomous mechanism.[11] Essentially, most studies attributed the anti-obesity effect of fermented dairy products to specific metabolites derived from milk fermentation or probiotics. Different dairy ingredients have varying effects on weight loss, including appetite reduction, inhibition of lipase activity and changes in the body's metabolic rate. However, detailed mechanisms and targeted strategies remain poorly understood.

Peptides derived from milk fermentation have drawn increasing attention as prominent ingredients of health-promoting functional foods targeted at diet-related chronic diseases.[12] These peptides display diverse activities affecting the digestive, immune, endocrine, cardiovascular and nervous system.[13] Therefore, they may contribute to lower the risk of obesity conferred by dairy consumption. For example, a

Nanjing Maternal and Child Health Institute, Women's Hospital of Nanjing Medical University, Nanjing Women and Children's Healthcare Hospital, 123 Tianfei Alley, Mochou Road, Nanjing, China. E-mail: chenboji@njmu.edu.cn, xwcui@njmu.edu.cn, chixia2001@njmu.edu.cn

†Electronic supplementary information (ESI) available. See DOI: https://doi.org/10.1039/d3fo05704f

‡These authors contributed equally to this work.

milk-derived peptide, Val-Pro-Pro, has been reported to improve inflammation and insulin sensitivity in obesity after oral administration.[14] VKEAMAPK named Miltin is an 8-amino acid peptide that matches bovine β-casein 98–105 aa,[15] which could be generated by fermentation.[16,17] Miltin is present in various dairy products such as infant formula, cheddar cheese, and fermented milk.[18] Specifically, Miltin, which originated from dairy food, is also present in human milk as a nonhuman peptide and may be absorbed by infants.[18,19] The common presence of Miltin in dairy products and its potential to resist gastrointestinal digestibility imply its importance. However, as Miltin has been simply identified for its antioxidant properties thus far,[15] the pursuit of exploring its other biological functions continues.

In the present study, we uncovered the function of Miltin in promoting thermogenesis in both brown and white adipose tissues, which caused a significant elevation in total body energy expenditure and resulted in resistance to diet-induced obesity and insulin resistance. We further found that Miltin induced the mitogen-activated protein kinase (MAPK) signaling pathway by interacting with DNA-damage-inducible protein 45 γ (GADD45γ). These data indicate that Miltin is a positive regulator in the thermogenic grogram and could represent a practical pharmacological approach to combat obesity.

2. Materials and methods

2.1. Peptide synthesis

The synthesized Miltin with a minimum purity of 95% was obtained from Science Peptide Biological Technology Co., Ltd, GenScript (Shanghai, China). The synthesized Miltin was dissolved in PBS at a stock concentration of 100 mM, aliquoted, and stored at −80 °C until further use.

2.2. Animal experiments

Male C57BL/6J mice were purchased from the Animal Core Facility of Nanjing Medical University. All animal procedures were approved by the Nanjing Medical University Committee on the Care and Use of Animals (permit number IACUC-1803023). For the adaptive thermogenesis study, mice were intraperitoneally (i.p.) injected with the synthesized Miltin peptide or an equivalent amount of normal saline as the vehicle daily for 2 weeks. The cold exposure experiment was performed at 4 °C with free access to food and water. For the obesity reversal study, mice were maintained on a high-fat diet (HFD) (60% calorie from fat, research diet) for 6 months before initiating injections. The diet-induced obesity (DIO) mice were administered with an i.p. injection of either saline or Miltin (10 mg kg^{-1}) daily for the next 2 months. For the obesity-prevention study, mice were fed with an HFD for 10 weeks. Miltin was administered at 5 mg kg^{-1} and 10 mg kg^{-1} i.p. twice a week during the HFD period. To study the effect of early Miltin exposure on the thermogenic capacity of pups, littermates were separated into two groups and treated with Miltin or vehicle by oral gavage separately. The body mass and food intake amounts were monitored daily or each week. Animals were sacrificed at indicated time points, and blood and tissue samples were harvested for molecular biology, histology, and biochemistry analyses.

2.3. Temperature measurements and indirect calorimetry

The rectal body temperature was measured using a BAT-12 microprobe thermometer (Physitemp Instruments Inc., Clifton, NJ, USA). Skin temperatures were recorded using an infrared camera (Thermo GEAR G120/G100, NEC Avio Infrared Technologies Co., Ltd, Tokyo, Japan). Individual VO_2, VCO_2, locomotor activity and heat production were determined using a TSE PhenoMaster system (TSE Systems GmbH, Bad Homburg, Germany) at ambient temperature. The parameters of oxygen consumption (mL kg^{-1} h^{-1}), carbon dioxide production (mL kg^{-1} h^{-1}) and RER (CO_2/VO_2) were calculated for each mouse divided by its body weight. Mice were allowed *ad libitum* access to food and water during measurements.

2.4. *In vitro* oxygen consumption

Brown and white pre-adipocytes were plated and differentiated in XF 24-well microplates (Seahorse Bioscience) at 37 °C in an atmosphere containing 5% CO_2. Cellular oxygen consumption rate (OCR) was determined using a Seahorse Bioscience XF24 analyzer (Agilent Technologies, CA, USA), as described previously.[20] ATP synthase inhibitor oligomycin (1 μM), mitochondrial uncoupler carbonyl cyanide 4-(trifluoromethoxy)phenylhydrazone (FCCP, 1 μM) and the electron transport inhibitor rotenone (0.5 μM) were injected sequentially. The OCR was calculated using the Seahorse XFp Analyzer software (Agilent Technologies).

2.5. PET/CT

PET/CT imaging was performed using an Inveon micro-PET/CT scanner (Siemens Medical Solution, Germany). After administration with Miltin for 2 weeks, mice were fasted overnight and were injected with ^{18}F-fluorodeoxyglucose (FDG) under isoflurane anesthesia. Ten-minute static PET scans were acquired at 30 min post-injection, and then CT images were analyzed at 40 min after FDG injection. The PET data were reconstructed using a three-dimensional (3D) ordered subset expectation maximization algorithm (OSEM3D) with CT-based attenuation and scatter correction. The quantification of FDG uptake was done by manually circling the regions of interest over areas containing BAT according to the CT images.

2.6. *In vivo* imaging

N-terminal fluorescein isothiocyanate (FITC)-labeled Miltin was administered into mice at a dose of 100 mg per kg body weight *via* i.p. injection. Mice were anesthetized with isoflurane, and the fluorescence intensities were determined at 3 h after administration using an IVIS Spectrum Imaging System (Xenogen, Alameda, CA, USA). The accumulation of FITC-labeled Miltin was visualized in excised tissues, including the

heart, liver, spleen, kidney, inguinal WAT (iWAT), epididymal WAT (eWAT), BAT and muscle.

2.7. Proteome microarray assay and data analysis

A HuProt™ human proteome microarray analysis was performed by Shanghai Biotechnology Corporation (Shanghai, China). The microarrays were blocked with 5% bovine serum albumin in phosphate-buffered saline with 0.1% Tween (PBST) for 1.5 h at room temperature. Biotinylated Miltin diluted in a blocking buffer was incubated with the blocked protein microarray at room temperature for 1 h. The microarray was washed three times with PBST for 10 min and then probed with a 0.1% Cy5-streptavidin solution at room temperature for 20 min, followed by three 5 min washes in PBST. The microarray was spun dry at 1000*g* for 2 min and scanned using a GenePix 4000B scanner (Axon Instruments, USA). The data were processed using GenePix Pro v6.0 (Axon Instruments, USA).

2.8. Biotin pull-down assays

Human brown adipocyte lysates used for the peptide pull-down assays were prepared in a RIPA buffer. Next, 20 μL immobilized streptavidin beads (Dynabeads M-280 streptavidin, Invitrogen) were loaded with 50 μg biotinylated peptide for incubation with cell lysates. Approximately 1 mg lysate was incubated with the peptide at 4 °C for 12 h, and then the beads were pelleted with a magnet for 2–3 min. After extensive washes in Tris-buffered saline with 0.1% Tween, bound proteins were eluted by boiling in a 1 × loading buffer. Eluates from the bait peptide pull-downs were loaded into an SDS-PAGE gel for western blot detection of GADD45γ (PA5-112425, Invitrogen). Total brown adipocyte lysates were also loaded together as a positive control.

2.9. Biolayer interferometry binding assays

The interaction between Miltin and GADD45γ was determined using a ForteBio Octet Red system (ForteBio, Inc). Wild-type and mutant recombinant His-tagged GADD45γ were immobilized on Ni-NTA biosensors (Sartorius) until saturation, and the peptide–protein association and dissociation were monitored for 400 s. Data were processed using the ForteBio Data Analysis Software.

2.10. Statistical analysis

Data are presented as mean ± SD. Comparisons between groups were evaluated using Student's *t*-test or one-way ANOVA when indicated. Statistical significance was defined as $^{*}P < 0.05$ and $^{**}P < 0.01$ *versus* controls.

3. Results

3.1. Identification of Miltin as a thermogenic activator

We have previously reported that antioxidant supplementation could attenuate oxidative stress and prevent H_2O_2-induced decline in the thermogenic function of brown adipocytes.[21] Since Miltin was identified for its antioxidant capacity, we thus evaluated its effect on thermogenesis regulation in adipocytes. Immunofluorescence confocal microscopy showed that FITC-labeled Miltin successfully entered adipocytes (ESI Fig. S1A†). We then examined its function in promoting cellular respiration by Seahorse assays. As shown in Fig. 1A, the mitochondrial respiratory capacity of mature brown adipocytes was remarkably elevated in the presence of Miltin, as indicated by the basal OCR, proton leak, ATP production and maximal respiration. Furthermore, mRNA expression levels of brown adipocyte hallmark genes (Ucp1, Pparα, Pgc1α, Dio2 and Cidea) were significantly induced (Fig. 1B). Accordingly, the UCP1 protein level was markedly upregulated in response to Miltin stimulation (Fig. 1E). This was also supported by results from mature white adipocytes treated with Miltin showing elevated energy expenditure and increased expression of thermogenic genes (Fig. 1C, D and F). These findings indicated that Miltin induces the thermogenic program in differentiated brown and white adipocytes.

To further test whether the activation of adipocyte thermogenesis by Miltin treatment promotes adipogenesis, we treated pre-adipocytes with Miltin during adipogenic differentiation. Oil Red O staining and triglyceride (TG) content detection revealed that chronic Miltin treatment did not alter the lipid accumulation or lipid droplet size present in the cells (Fig. S1B and S1C†). These suggested that Miltin directly promoted the thermogenesis of adipocytes rather than affecting their differentiation. We further found that Miltin has no significant effects on the cell viability of adipocytes, even at the highest dose (50 μM) (Fig. S1D†).

In summary, we identified a dairy milk protein-derived peptide, Miltin, that promoted adipocyte thermogenesis in a cell-autonomous manner.

3.2. Miltin activates thermogenesis in both BAT and WAT

Next, we assessed whether Miltin plays a role in regulating energy expenditure *in vivo*. We first attempted to monitor the biodistribution of Miltin by conjugating it to an FITC dye. As shown in ESI Fig. 2A,† a stronger fluorescence signal was detected in the liver, iWAT, and eWAT, and to a lesser extent in the kidney and BAT. These data suggested that Miltin successfully entered adipose tissue and may contribute to energy expenditure. C57BL/6J mice fed with a chow diet were then administered with Miltin or vehicle daily for 2 weeks. However, Miltin exposure did not markedly affect the body weight gain and food intake (Fig. 2A and ESI Fig. S2B†), nor the serum levels of glucose, insulin and TG under fasting conditions (ESI Fig. S2C†). Of note, we observed that the drop in body temperature was markedly delayed in Miltin-treated mice compared with the vehicle controls when performing a cold tolerance test (Fig. 2B). In accordance with this, Miltin administration increased the skin temperature, especially the BAT surface (interscapular), either at room temperature or upon exposure to 4 °C for 3 h, following a 2-week treatment (Fig. 2C). These results demonstrated that Miltin was able to increase thermogenesis to combat cold stress.

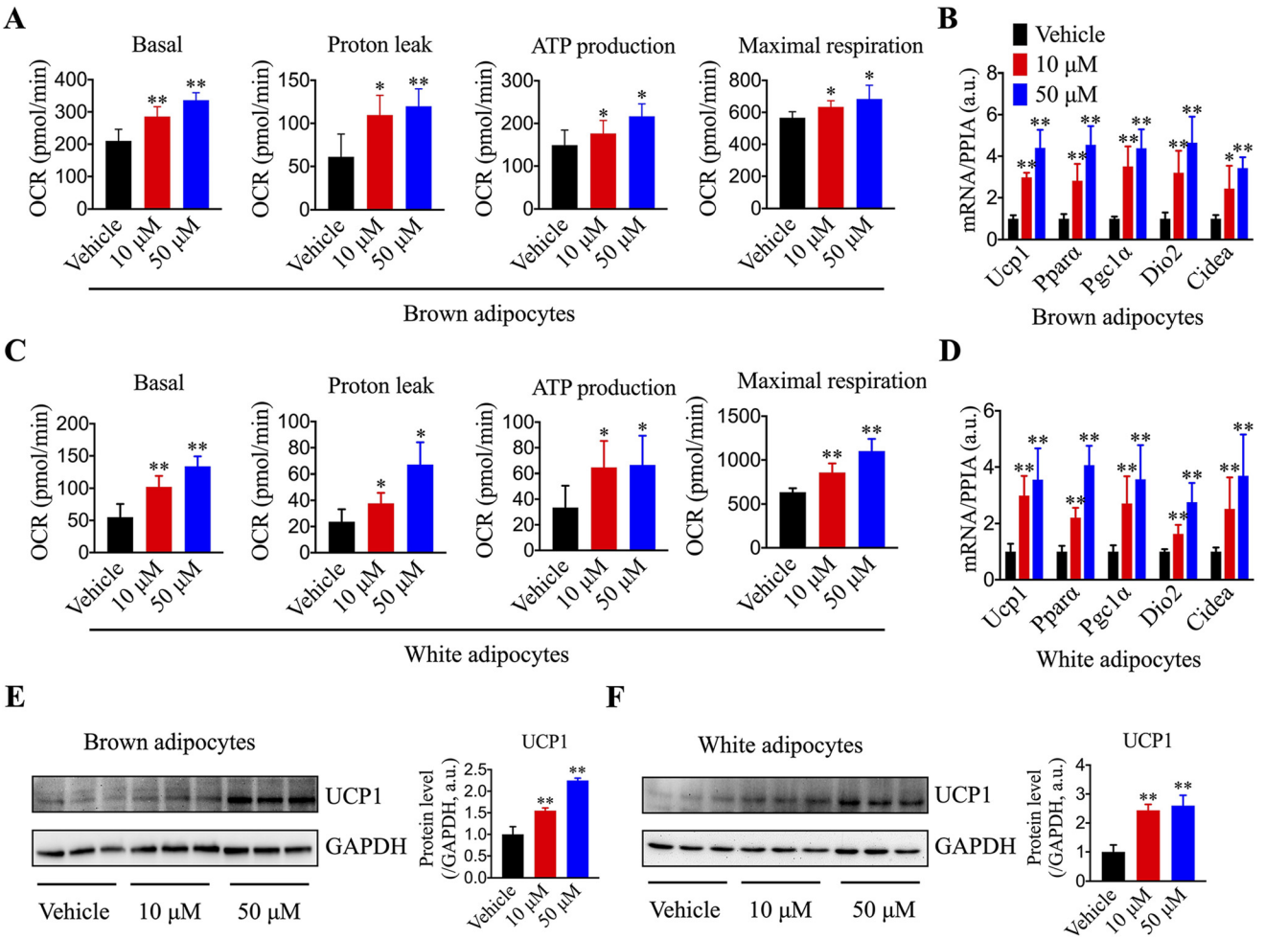

Fig. 1 Identification of Miltin as a thermogenic activator. (A) Oxygen consumption rates (OCRs) were measured using a Seahorse analyzer in mature brown adipocytes treated with or without Miltin for 3 h. Basal OCR, proton leak, ATP production and maximal respiration were quantified. (B) mRNA levels of thermogenic genes in mature brown adipocytes. (C and D) Energy expenditure and thermogenic gene levels were also evaluated in mature white adipocytes treated with or without Miltin for 3 h. (E and F) Immunoblots of UCP1 (left) and band intensity quantification normalized to loading control GAPDH (right) in mature brown and white adipocytes. Data are presented as mean ± SD. $*P < 0.05$ and $**P < 0.01$ *versus* vehicle, two-tailed unpaired Student's *t*-test.

PET/CT with ^{18}F-FDG is a reliable tool to image the activated brown adipocytes with heightened glucose uptake for thermogenesis. Our results of this study showed that ^{18}F-FDG uptake of interscapular BAT was prominently increased in Miltin-treated mice (Fig. 2D). Moreover, 3D reconstruction analyses also demonstrated the augmented uptake of ^{18}F-FDG in Miltin-treated mice (Movies, 1 and 2†). Coinciding with these, hematoxylin and eosin (H&E) staining showed strong UCP1 protein expression, as indicated by immunohistochemistry examination (Fig. 2E), although no histological change was detected in BAT and iWAT after the Miltin challenge. Other tissues including the brain, heart, liver, spleen, kidney, pancreas, muscle and intestine were also not histologically different in Miltin-treated mice, indicating its low biological toxicity (ESI Fig. S2D†). No significant difference was observed in the levels of the liver damage biomarkers alanine aminotransferase (ALT) and aspartate aminotransaminase (AST) (ESI Fig. S2E†). Moreover, the mRNA levels of Ucp1 and other thermogenic markers such as Pparα, Pgc1α, Dio2 and Cidea were strongly induced by Miltin (Fig. 2F). Western blot analysis indicated that the UCP1 protein expression levels were elevated in both BAT and iWAT from Miltin-treated mice compared with the vehicle controls (Fig. 2G). Together, these results suggest that Miltin could efficiently activate thermogenesis in BAT and induce iWAT browning.

Additionally, scrambled peptides (MPKAAVEK) were synthesized, and mice were treated with these peptides under the same paradigm to determine whether the function of Miltin was sequence specific. As shown in ESI Fig. S2F,† scrambled peptide-treated mice did not show better tolerance to cold exposure than vehicle-treated controls. These mice also failed to mount a robust thermogenic response neither at room temperature nor after cold exposure (ESI Fig. S2G†).

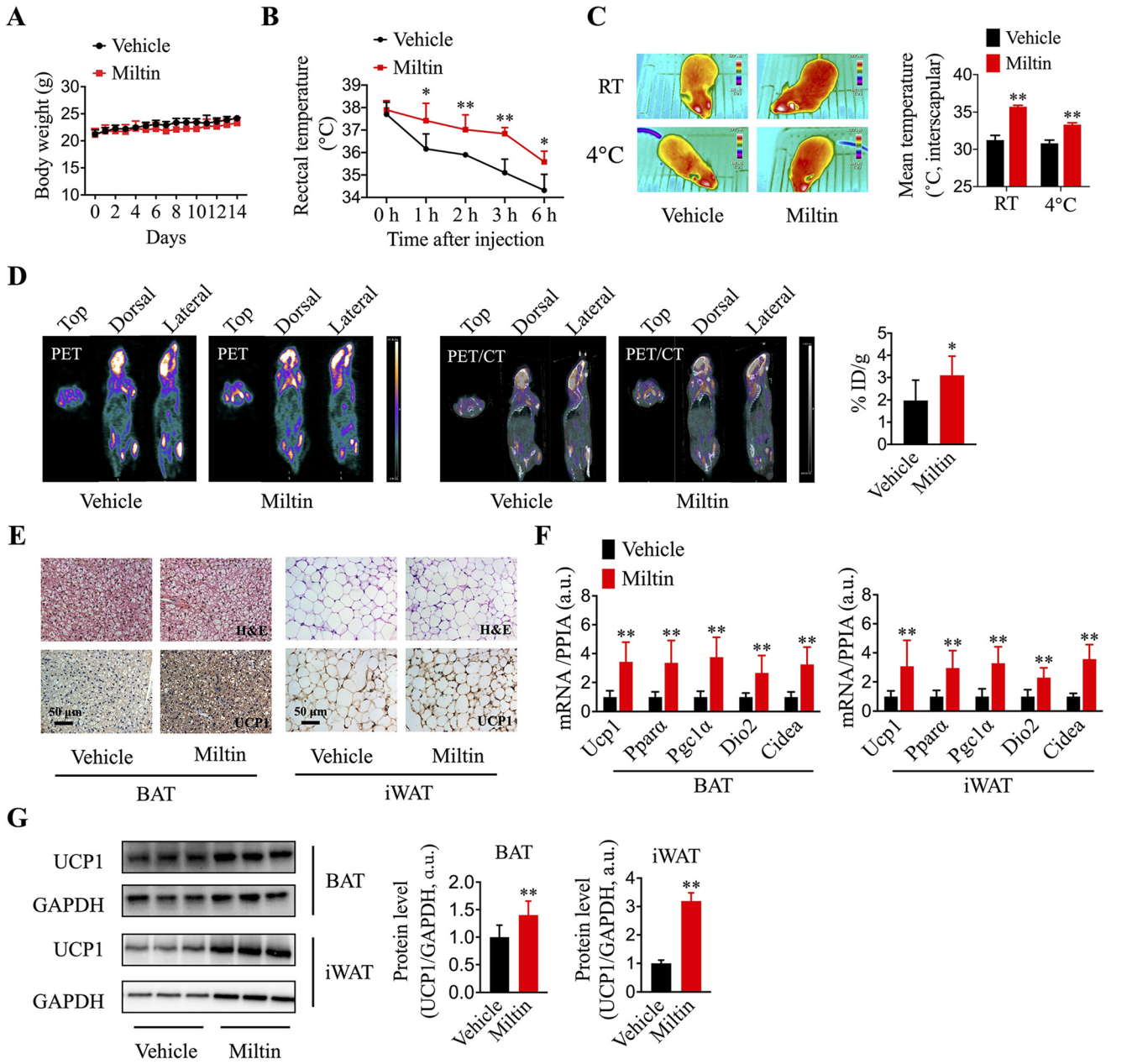

Fig. 2 Miltin activates thermogenesis in both BAT and WAT. Mice fed with a chow diet were administered an i.p. injection of 10 mg kg^{-1} Miltin or vehicle daily for 2 weeks (n = 5 per group). (A) Body weight changes in mice during the 2 weeks. (B) Rectal body temperature of mice housed at 4 °C. (C) Representative infrared images of mice housed at 25 °C or 4 °C for 3 h after Miltin or vehicle injection. (D) Representative PET/CT images of mice treated with or without Miltin, and *ex vivo* quantification of FDG uptake in BAT deposits is shown on the right. (E) Representative images from H&E staining and UCP1 immunohistochemical staining of BAT and iWAT deposits. (F) qPCR was performed to compare thermogenic gene expression. (G) Western blot analysis of UCP1 protein expression in BAT and iWAT deposits. Band intensity quantification of western blot in BAT and iWAT deposits (right). Data are presented as mean ± SD. *P < 0.05 and **P < 0.01 *versus* vehicle, two-tailed unpaired student's t-test.

3.3. Miltin reverses diet-induced obesity by increasing energy expenditure

We further evaluated the pharmacological potential of Miltin in obesity treatment. Mice were fed with an HFD for 6 months to establish a DIO model and then randomly divided into two groups with a comparable body weight prior to Miltin or vehicle treatment. Intriguingly, the body weights and fat mass of the mice were significantly reduced after 2 months of Miltin treatment (Fig. 3A and B). Accordingly, the iWAT and eWAT fat pads were remarkably smaller in Miltin-treated animals than in control mice (ESI Fig. S3A†), demonstrating that Miltin treatment reversed diet-induced obesity. The lean mass and cumulative food intake were similar in both groups (ESI

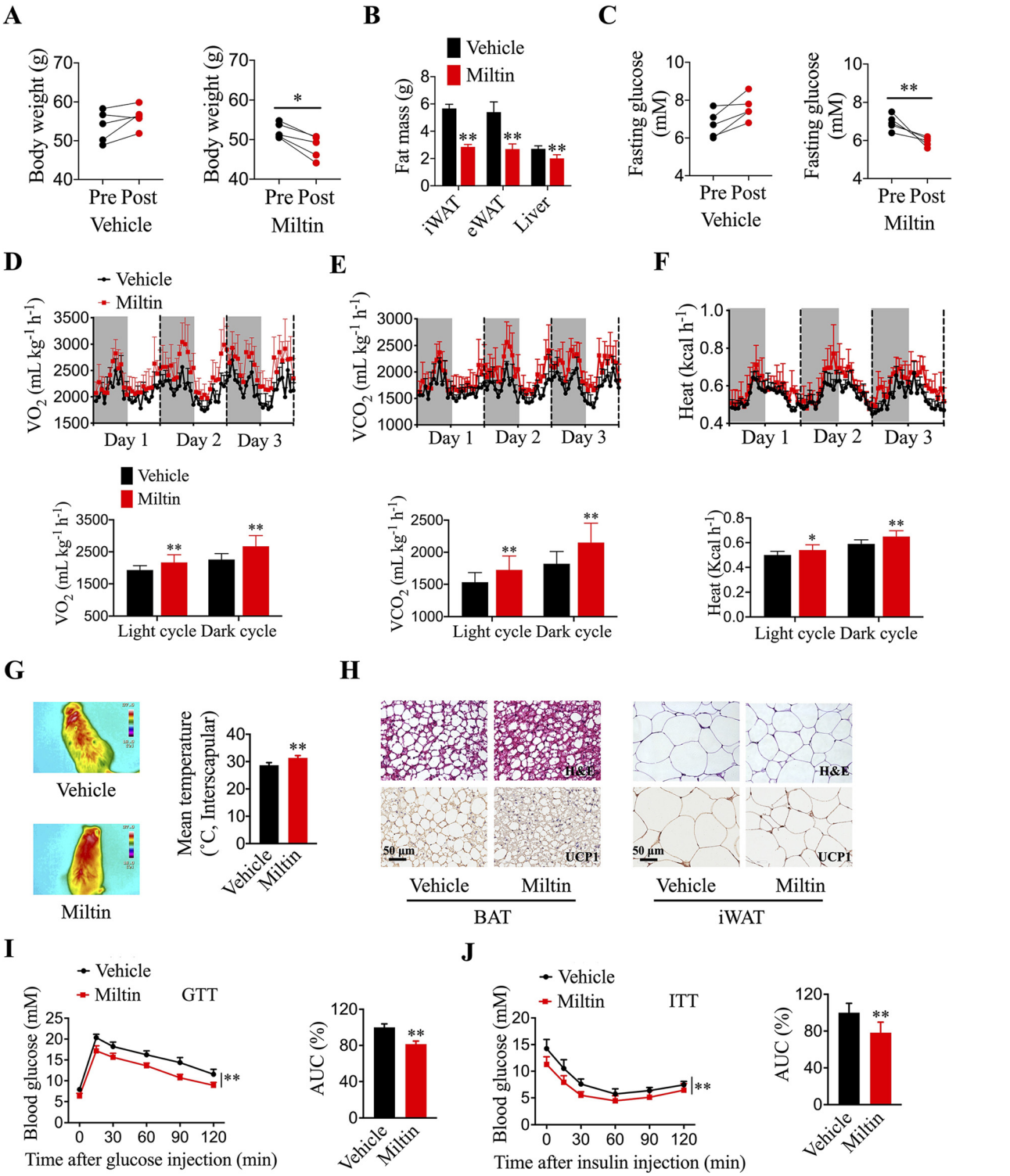

Fig. 3 Miltin reverses diet-induced obesity by increasing energy expenditure. Six- to eight-week-old C57BL/6J mice were maintained under an HFD for 6 months and then administered with Miltin or vehicle for a period of 8 weeks (n = 5 per group). (A–C) Body weight (A), body composition (B) and fasting glucose (C) changes in diet-induced obesity (DIO) mice pre- and post-Miltin (10 mg kg^{-1}) or vehicle treatment (n = 5 per group). (D–F) O_2 consumption (D), CO_2 production (E) and heat generation (F) were measured in metabolic cages between the Miltin-treated group and the vehicle control (top, n = 6 per group). The gray part indicates the dark phase. Average O_2 consumption, CO_2 production and heat generation in dark and light phases are indicated on the bottom. (G) Representative infrared images of DIO mice injected with Miltin or vehicle (left, n = 5 per group). quantitation of mean skin temperature on the interscapular area (BAT) after 2-month Miltin treatment or vehicle injection (right). (H) Representative images of H&E staining and UCP1 immunohistochemistry staining in BAT and iWAT of DIO mice. (I and J) GTT and ITT were performed before body weight showed the difference. Data are presented as mean ± SD. *P < 0.05 and **P < 0.01 *versus* vehicle, two-tailed unpaired Student's t-tests (A–G). **P < 0.01, one-way ANOVA (I and J).

Fig. S3B and 3C†), suggesting that the changes in body weight exclusively resulted from decreased fat mass (43.7%). Of note, serum levels of glucose under fasting conditions as well as TG and insulin were also robustly reduced in mice with Miltin treatment when compared with vehicle controls (Fig. 3C and ESI Fig. S3D†). Notably, Miltin treatment induced significantly elevated oxygen consumption (VO_2), CO_2 production (VCO_2) and heat generation (Fig. 3D–F). The respiratory exchange ratio (RER) was determined by dividing VCO_2 produced by VO_2 consumed. Compared with the control, the Miltin-treated mice exhibited higher RER values in both dark and light phases (ESI Fig. S3E†), indicating an altered substrate utilization to preferentially utilize carbohydrates over lipids after Miltin had reduced fat mass. In contrast, total locomotor activity appeared comparable between the two groups (ESI Fig. S3F†).

To explore whether these body weight losses and elevated energy expenditure were due to the contribution of Miltin to thermogenic capacity, we measured the heat production in control and Miltin-treated mice, mainly in BAT and iWAT. Miltin increased the interscapular skin temperature compared with vehicle injection in control mice (Fig. 3G). Similarly, histological analysis showed strongly decreased fat accumulation and strikingly increased staining with an antibody recognizing UCP1 in an immunological assay of Miltin-treated mice (Fig. 3H). At the molecular level, the protein level of UCP1 was consistently increased (ESI Fig. S3G†). Moreover, glucose tolerance tests (GTTs) and insulin tolerance tests (ITTs) indicated that Miltin treatment significantly improved glucose tolerance and insulin sensitivity (Fig. 3I and J). These results together demonstrated that the enhancement of adipose thermogenesis mainly accounts for body weight loss and elevated energy expenditure in Miltin-treated mice under HFD exposure.

3.4. Miltin protects against diet-induced obesity and improves glucose homeostasis

In addition to its therapeutic action on obesity, we also examined whether Miltin was able to prevent diet-induced fat gain. Male C57BL/6J mice fed with an HFD for 10 weeks were treated with either Miltin or vehicle twice weekly. The body weight gain of the Miltin-treated mice at 10 mg kg^{-1} began to slow down from 7 weeks onwards without changing food intake compared to controls, with lower doses showing a delayed effect (Fig. 4A and ESI Fig. S4A†). We further revealed that the slowed body weight gain resulted from the strong reduction in adiposity (iWAT and eWAT), and not in lean mass (Fig. 4B–D), indicating the resistance to HFD-induced obesity. As expected, Miltin-treated mice exhibited dose-dependent reductions in fasting blood glucose, as well as lowered circulating blood insulin and TG levels (Fig. 4E and F). These mice also showed improved glucose and insulin tolerance (Fig. 4G and H). Histological staining revealed that both the BAT and iWAT showed increased brown adipose appearance (less lipid storage and hypertrophy and increased UCP1 content) in response to the Miltin treatment (Fig. 4I). In support of this, the protein expression level of UCP1 was dramatically increased in BAT and iWAT from Miltin-treated mice (ESI Fig. S4B†). Moreover, a significant but weaker impact of Miltin on O_2 consumption, CO_2 production, heat generation, and RER was observed in Miltin-treated mice in comparison with vehicle controls, while these changes were not related to the locomotor activity (ESI Fig. S4C–4G†). We also observed an obvious increase in body temperature following the Miltin treatment (Fig. 4J and ESI Fig. S4H†).

3.5. Miltin-mediated thermogenesis is MAPK dependent

To investigate the underlying molecular pathways accounting for Miltin-mediated increased thermogenesis, we performed RNA sequencing (RNA-seq) to identify the differentially expressed genes in mature brown adipocytes treated with Miltin compared with the vehicle control. A total of 550 genes showed significant differences between these two groups, with 235 upregulated and 315 downregulated (ESI Fig. S5A†). Additionally, the hierarchical clustering of the expression profiles of 550 genes perfectly segregated between Miltin and the vehicle control (ESI Fig. S5B†). The Kyoto Encyclopedia of Genes and Genomes (KEGG) analysis based on the transcriptomics displayed the top 30 pathways significantly regulated by Miltin treatment (Fig. 5A). Of these pathways, the MAPK signaling pathway presented the highest enrichment score, and its family members were extensively impacted by Miltin. Therefore, the MAPK pathway may be responsible for Miltin-induced thermogenesis in adipocytes.

We then examined the activation of MAPK subfamilies involved in adipocyte energy homeostasis: Jun amino-terminal kinase (JNK1/2), extracellular signal-regulated kinases (ERK1/2) and p38 kinases (p38).[22] As shown in Fig. 5B, phosphorylated JNK1/2, ERK1/2 and p38 were dose-dependently increased in both brown and white adipocytes after Miltin treatment. Consistently, enhanced phosphorylation of ATF2 and CREB as well as PGC1α protein levels were observed following Miltin treatment (ESI Fig. S5C and S5D†). The results were further verified by western blot analyses in BAT and iWAT tissues from chow-fed mice treated with Miltin for 2 weeks (ESI Fig. S5E–S5H†). The quantification for the western blot results of MAPK events is summarized in ESI Fig. S6.† Inhibitors of JNK (SP600125), ERK1/2 (U0126), and p38 (SB203580) were used to explore whether the activation of MAPK members was responsible for Miltin-mediated thermogenic events. Pilot experiments showed that pretreatment of cells with inhibitors reduced the Miltin-induced phosphorylation of JNK1/2, ERK1/2 and p38 (ESI Fig. S7A and S7B†). Moreover, the upregulation of UCP1 proteins induced by Miltin was remarkably blocked in brown and white adipocytes pretreated with these three inhibitors (Fig. 5C, D, ESI Fig. S7C and S7D†). These data strongly suggested that the Miltin-induced thermogenesis in adipocytes was mediated *via* the activation of MAPK pathways.

3.6. GADD45γ is responsible for Miltin-mediated thermogenesis

To explore the direct binding protein of Miltin, a proteome microarray analysis was performed with 19 851 GST-tagged human proteins. Miltin and the scrambled peptide were biotiny-

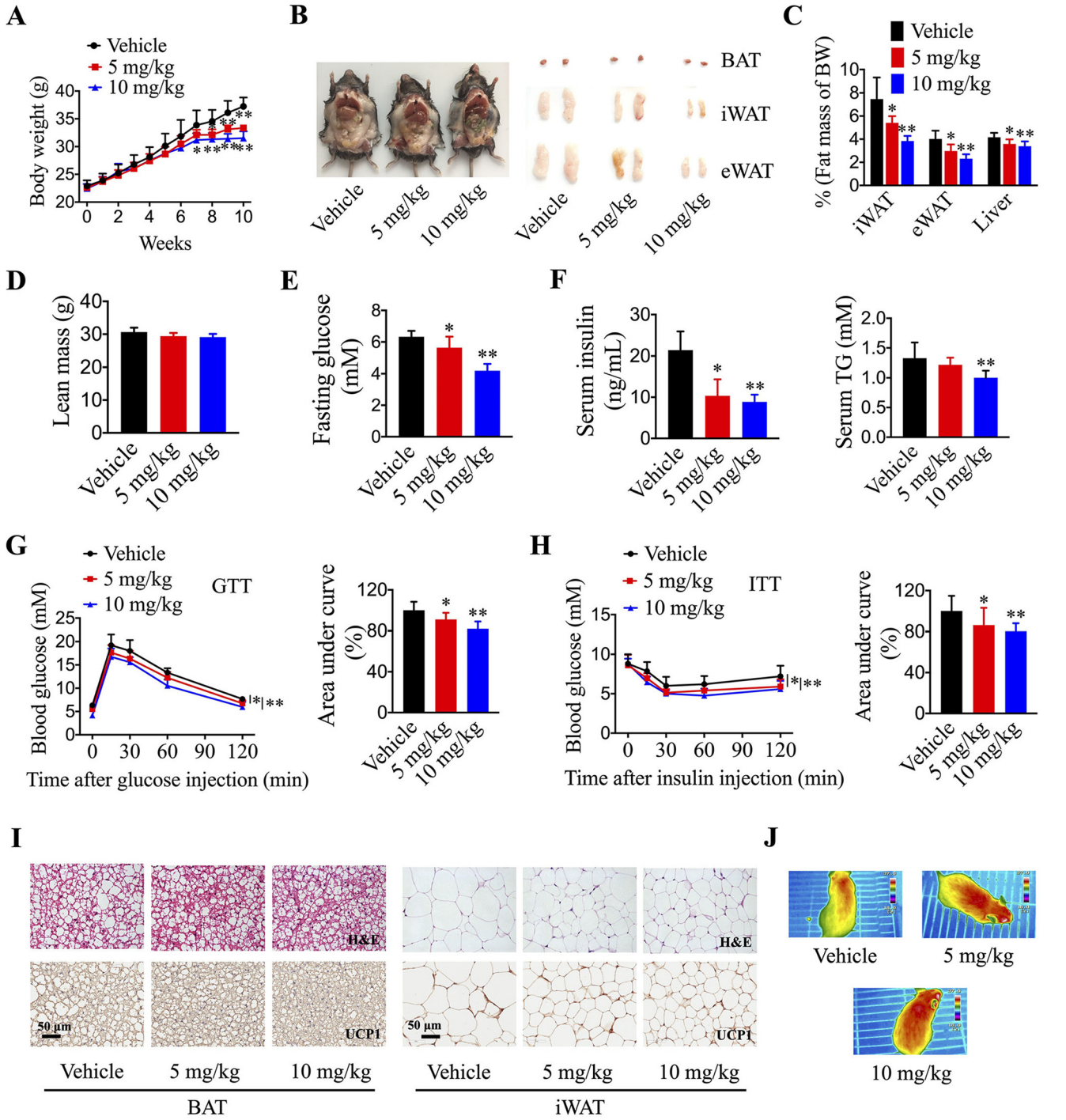

Fig. 4 Miltin protects against diet-induced obesity. Six- to eight-week-old C57BL/6J mice maintained under an HFD were injected with Miltin or vehicle at doses of 5 mg kg^{-1} and 10 mg kg^{-1} twice per week for a period of 10 weeks (n = 7 per group). (A) Body weight of mice injected with Miltin or vehicle during HFD feeding. (B) Representative pictures of HFD-fed mice (left) and excised BAT, iWAT and eWAT deposits (right). (C) Quantification of BAT, iWAT and eWAT deposits of HFD-fed mice. (D) Lean mass of mice. (E and F) Serum levels of fasting glucose (E) as well as insulin and TG (F). (G and H) GTT and ITT were performed after 4 weeks of Miltin treatment. (I) Representative images of H&E staining and immunohistochemistry staining of UCP1. (J) Representative infrared images of mice. Data are presented as mean ± SD. *P < 0.05 and **P < 0.01 *versus* vehicle, two-tailed unpaired student's t-tests (A–F). *P < 0.05 and **P < 0.01, one-way ANOVA (G and H).

lated and probed on the microarray, and the Miltin-protein interactions were visualized with Cy5-conjugated streptavidin. We identified totally 148 candidate proteins that were specifically bound to Miltin after the removal of nonspecific signals as compared to the scrambled control (ESI Fig. S8A†). To gain insights into the functional roles of these potential target pro-

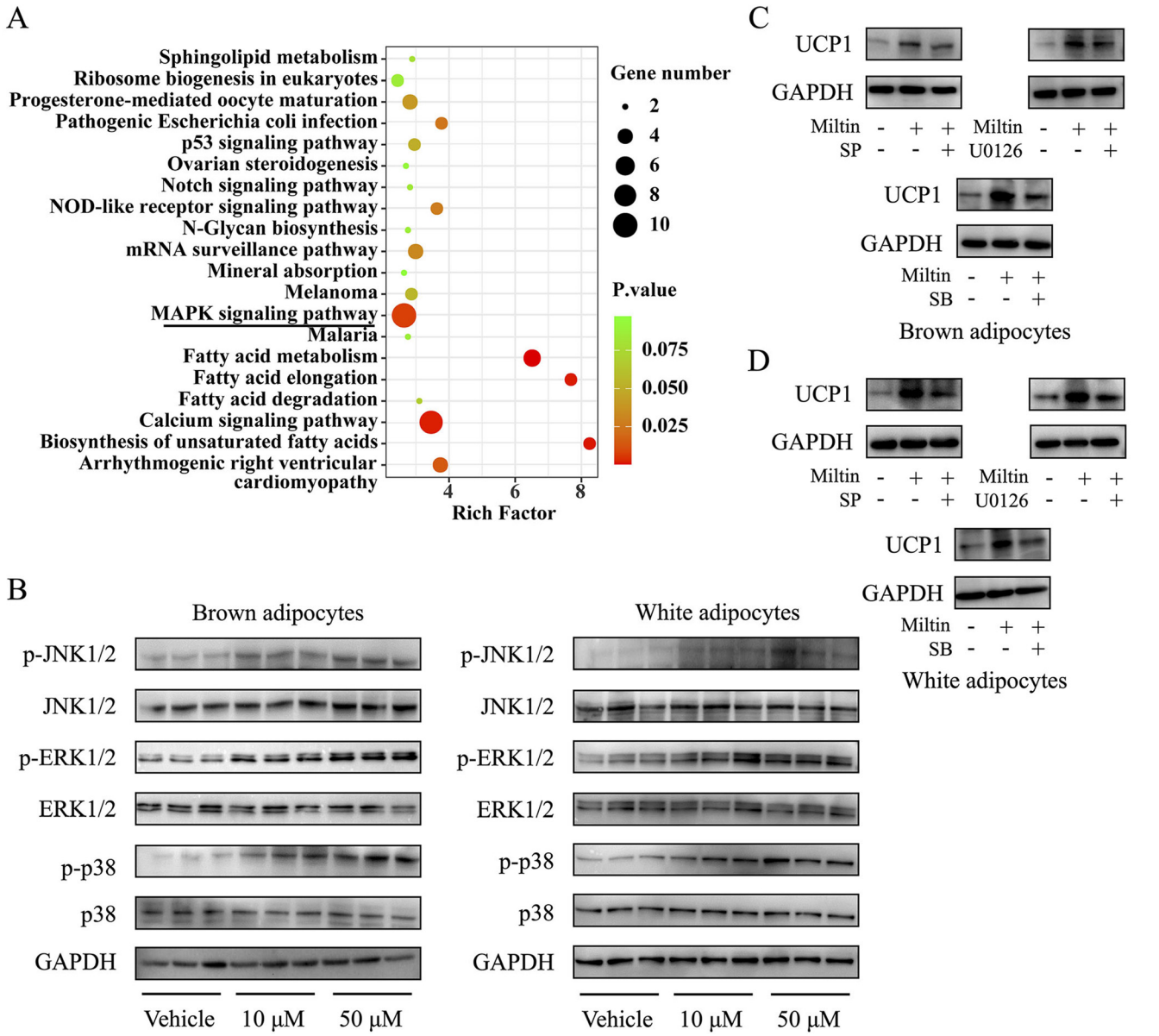

Fig. 5 Miltin-mediated thermogenesis is MAPK dependent. (A) Kyoto Encyclopedia of Genes and Genomes (KEGG) plot analysis showing the top 30 pathways regulated by Miltin treatment. (B) Immunoblots indicating phosphorylated and total protein levels of JNK, ERK1/2 and p38 in mature brown and white adipocytes treated with Miltin or vehicle control. (C and D) Immunoblots indicating UCP1 protein levels in Miltin-treated brown adipocytes (C) and white adipocytes (D) with or without the presence of JNK inhibitor SP600125, ERK1/2 inhibitor U0126 and p38 inhibitor SB203580 at a dose of 10 μM.

teins, the KEGG analysis was performed and the results showed substantial enrichment in the spliceosome, focal adhesion, and MAPK signaling pathways (ESI Fig. S8B†). Considering the causal relationship between Miltin and the MAPK pathway uncovered previously, we thus focused on the proteins involved in this signaling. As listed in ESI Fig. S8C,† the presence of GADD45γ attracted our attention. Numerous studies have shown the pivotal regulatory function of GADD45γ in activating the thermogenesis of BAT.[23,24] Accordingly, GADD45γ was selected as a potential target of interest for further study.

To validate the binding specificity between Miltin and GADD45γ, we performed a biolayer interferometry (ForteBio) assay. The dissociation constant (K_d) of Miltin for GADD45γ was 93.1 nM, while K_d for the scrambled peptide could not be determined as it failed to bind to the GADD45γ protein (Fig. 6A). Furthermore, a precipitation assay using a biotin–streptavidin system also revealed a direct interaction between Miltin and GADD45γ (ESI Fig. S9A†). To further characterize the Miltin-GADD45γ interaction, Molecular Operating Environment (MOE) 2019.0102 was used to predict possible binding sites and build a 3D structure of GADD45γ with Miltin. Molecular docking simulation showed that Miltin is preferably bound to GADD45γ residues Gln20 and Glu66 with an *S*-score of −7.47 kcal M^{-1} (Fig. 6B). The 3D structures

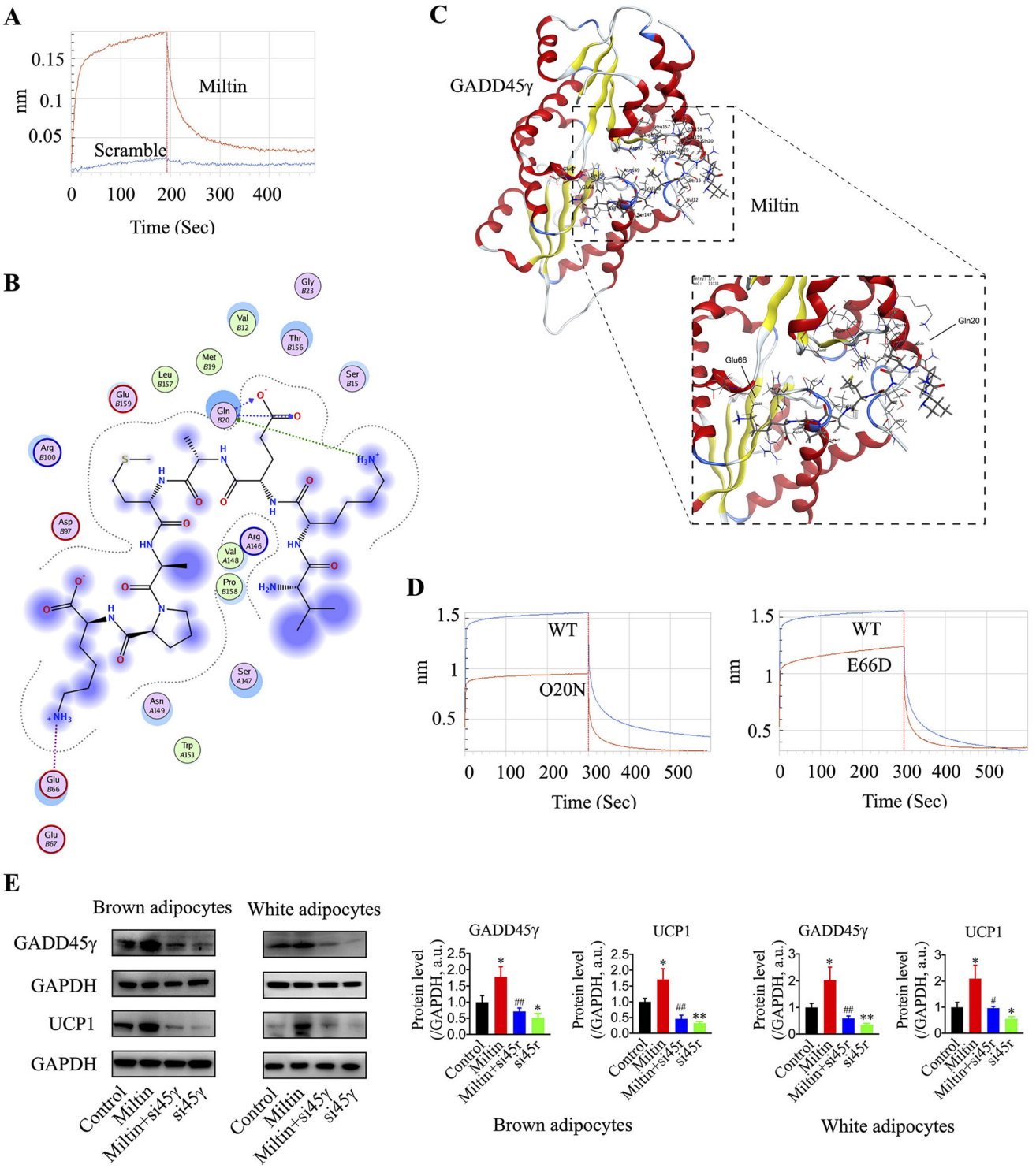

Fig. 6 GADD45γ is responsible for Miltin-mediated thermogenesis. (A) Kinetic binding curve for Miltin and GADD45γ determined by ForteBio Octet Red. (B) Two-dimensional view showing the amino acid residues of GADD45γ that are required to bind Miltin. (C) Three-dimensional view of the interaction between Miltin and the binding sites of GADD45γ using MOE. (D) Kinetic binding data for GADD45γ mutant proteins (Q20N and E66D) and Miltin. (E) Immunoblots indicating the protein levels of UCP1 in brown and white adipocytes transfected with siRNAs targeting GADD45γ in the presence of Miltin or not. Data are presented as mean ± SD. $^{*}P < 0.05$ and $^{**}P < 0.01$ *versus* control, $^{\#}P < 0.05$ and $^{\#\#}P < 0.01$ *versus* Miltin, two-tailed unpaired student's *t*-tests.

showed that Gln20 and Glu66 acted like two "spot rivets" that anchored Miltin together with GADD45γ (Fig. 6C). Moreover, sequence identity at the amino acid level revealed that these two sites were conserved within human and mouse genomes (ESI Fig. S9B†). To further confirm the binding specificity between Miltin and residues Gln20 and Glu66 in GADD45γ, we purified wild-type and mutant recombinant GADD45γ proteins produced in *E. coli* (ESI Fig. S9C†). Point mutations at Gln20 and Glu66 abolished the binding ability, suggesting the crucial roles of these positions for the interaction between Miltin and GADD45γ (Fig. 6D). Next, we questioned whether GADD45γ mediated Miltin-induced activation of UCP1 expression. The knockdown of GADD45γ was achieved by delivering small interfering RNA (siRNA) to human brown and white pre-adipocytes, and the deficiency was sustained throughout differentiation (Fig. 6E). We found by western blot analyses that the elevation of UCP1 expression stimulated by Miltin was attenuated in GADD45γ-knockdown adipocytes (Fig. 6E), implying the functional interaction between Miltin and GADD45γ. Consistent with this, oxygen consumption studies indicated that Miltin-induced energy expenditure *in vitro* was recovered by GADD45γ knockdown (ESI Fig. S10A and S10B†).

3.7. Miltin enhances GADD45γ stability by reducing its ubiquitination

How Miltin affected GADD45γ remained uncertain. Notably, the protein expression levels of GADD45γ were remarkably increased by Miltin in a dose-dependent manner *in vitro* (Fig. 7A). A similar pattern of GADD45γ expression was noticed in BAT and iWAT of mice injected with Miltin (ESI Fig. S10C†). In contrast, the GADD45γ mRNA abundance in Miltin-treated adipocytes was comparable with controls (Fig. 7B), pointing to the posttranscriptional regulation of Miltin. When inhibiting protein synthesis with cycloheximide (CHX), we found that Miltin increased GADD45γ protein stability in both brown and white adipocytes (Fig. 7C and D). These findings prompted us to consider that Miltin may function through inhibiting GADD45γ degradation. A previous study has proposed that GADD45 family members are labile proteins and prone to undergo constitutive ubiquitination and proteasome-dependent degradation.[25] We thus focused on the ubiquitin-proteasome pathway to uncover how Miltin led to an increase in GADD45γ protein stability. As expected, MG132, a proteasome inhibitor, significantly enhanced the protein level of GADD45γ in the absence or presence of Miltin (Fig. 7E). We further examined the ubiquitination changes of GADD45γ in 293T cells co-transfected with N-terminal hemagglutinin-tagged ubiquitin (HA-Ub) and GADD45γ, and observed low ubiquitination levels in the Miltin group when compared with the scrambled peptide control (Fig. 7F and ESI Fig. S10D†). Overall, these data suggested that Miltin functioned as a GADD45γ stabilizer by suppressing its ubiquitination and subsequent proteasomal degradation.

4. Discussion

Obesity, a worldwide public health issue, develops from the imbalance between energy intake and expenditure.[26] Targeting BAT thermogenesis or WAT browning to burn fat into heat represents a promising therapeutic strategy to combat obesity.[3] In this study, we showed that Miltin, a dairy-derived peptide, activates the thermogenic programs in brown and white adipocytes. The administration of the synthesized Miltin elevated the core body temperature and energy expenditure, and was able to prevent and reverse HFD-induced obesity. In addition to body weight loss, Miltin treatment evoked a substantial number of beneficial metabolic effects including reduced glucose and insulin levels as well as improved glucose tolerance and insulin sensitivity. Finally, we determined that Miltin promoted UCP1 expression and thermogenesis in a cell-autonomous manner by directly interacting with GADD45γ, specifically, by preferentially activating the MAPK signaling pathway.

Recently, much effort has been made to discover novel substances or molecules as anti-obesity drugs that enhance adipose tissue thermogenesis and metabolism.[27] Due to their inherent properties as drug molecules and technological advances in chemistry, peptides have drawn increased attention for anti-obesity drug development.[28,29] There is no better example than developing agonists for the glucagon-like peptide 1 (GLP-1) receptor, which stands as one of the highly successful classes of peptide drugs in diabetes and obesity treatment.[30] In addition, screening novel peptides has become a popular strategy for identifying new drugs against obesity. Lee C. *et al.* demonstrated that MOTS-c, a mitochondrial-derived peptide, promoted brown and white fat thermogenesis, thus contributing to anti-obesity effects.[31] In addition, a series of peptides such as Secretin and D3 (human α-defensin 5 modified peptide) also show great hope in fighting against obesity and its comorbidities.[32,33] In this study, we demonstrated that long-term Miltin administration mitigated diet-induced obesity and related co-morbidities including glucose intolerance and insulin resistance in mice. Given the potent anti-obesity effects in rodents, repurposing Miltin in clinical settings could represent a new pharmacological approach to treating obesity and its metabolic comorbidities.

With accumulating evidence confirming the obesity-prevention outcome of breastfeeding, many milk components such as fibroblast growth factor (FGF21) regarded as improving offspring metabolic outcomes were identified in human milk.[34–37] A remarkable increase in energy metabolism accompanies the sudden shift from the fetus to the neonate; for example, postnatal brown fat thermogenesis increases rapidly after birth to keep the newborn warm. As a well-known thermogenic regulator, the circulating level of FGF21 is increased by sucking and injecting FGF21 into neonatal mice resulting in enhanced expression of thermogenic genes in BAT.[37,38] Moreover, the signaling lipids present in human milk have recently emerged as hormones to regulate metabolic phenotypes in offspring.[39] For example, alkylglycerol (AKG) increased the beige adipocyte content in infants in an adipose tissue

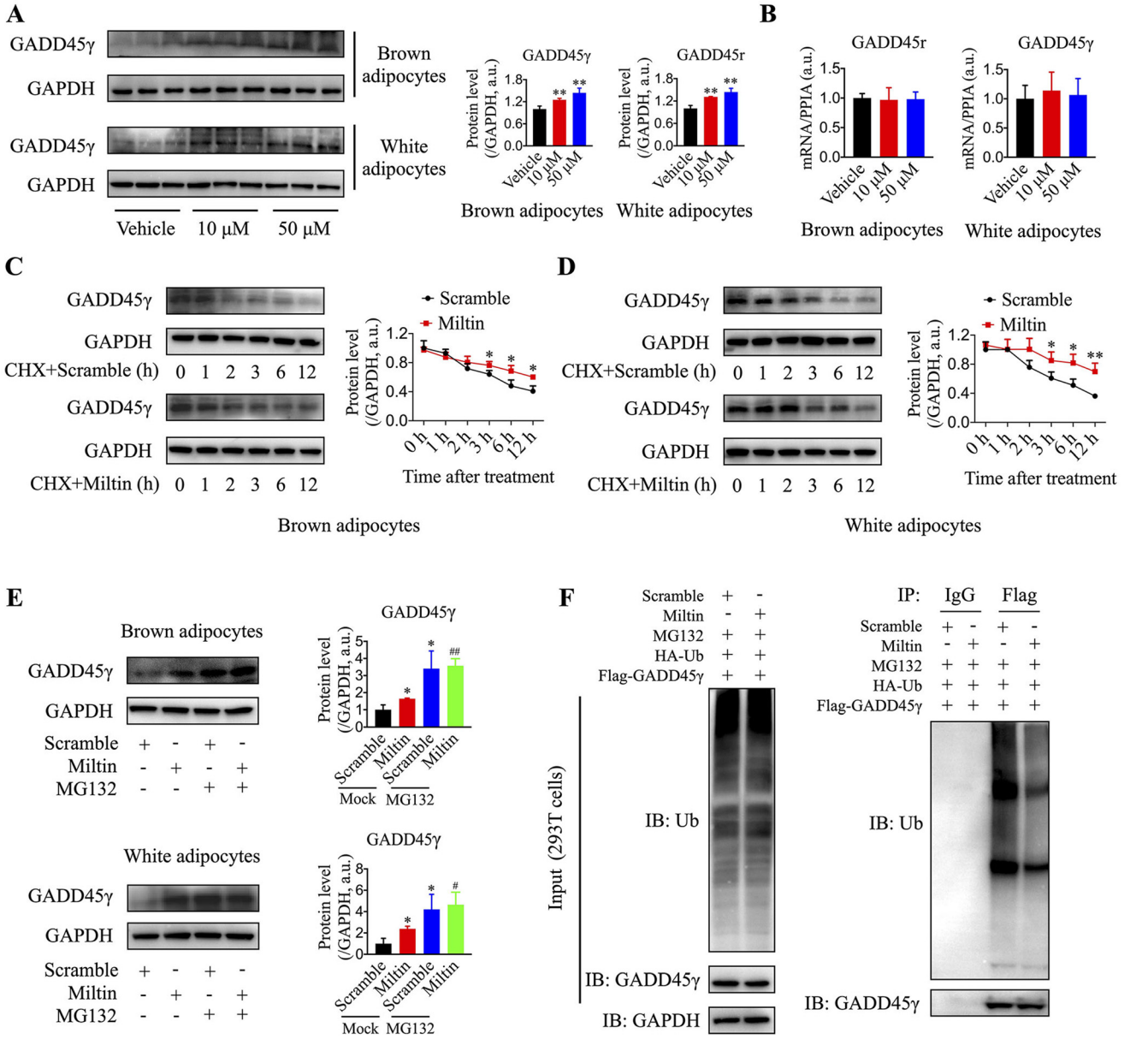

Fig. 7 Miltin enhances GADD45γ stability by reducing its ubiquitination. (A) Immunoblots showing the protein levels of UCP1 in brown adipocytes and white adipocytes treated with Miltin (left). Band intensity quantification of UCP1 normalized to GAPDH control (right). (B) Relative mRNA levels of UCP1 in Miltin-treated adipocytes. (C and D) Degradation of GADD45γ in brown and white adipocytes. Cells were treated with 10 μg mL^{-1} cycloheximide (CHX) alone or together with Miltin or scrambled peptides for the indicated time. (E) MG132 contributed to GADD45γ accumulation in brown and white adipocytes. Cells treated with Miltin or scrambled control were incubated with 50 μM MG132 for 24 h, and then the levels of GADD45γ were detected by western blot. (F) Ubiquitination assays exploring the ubiquitination of exogenous GADD45γ in 293T cells transfected with HA-Ub and FLAG-GADD45γ, with or without Miltin treatment. Data are presented as mean ± SD. $^{*}P < 0.05$ and $^{**}P < 0.01$ *versus* vehicle or scramble, $^{\#}P < 0.05$ and $^{\#\#}P < 0.01$ *versus* Miltin, two-tailed unpaired student's *t*-tests.

macrophage-dependent manner.[40] This process is extremely important for obesity prevention as white adipocytes progressively replace beige adipocytes in late infancy and adolescence,[4] while premature loss of beige adipocytes was linked to the development of obesity.[41] Miltin, which originated from dairy milk protein, is present in human milk and may be absorbed by infants.[18,19] Consistent with these findings, we also detected Miltin in both whole milk and human milk with mean concentrations of 27.9 ng mL^{-1} (range 10.17–51.39 ng mL^{-1}) and 1.26 ng mL^{-1} (range 0.74–1.84 ng mL^{-1}), respectively. We thus speculated that Miltin may also affect adipose tissue thermogenesis in infants and further provide a long-term protective mechanism against obesity.

Our results revealed that the Miltin-induced effects on adipocytes are, at least in part, mediated by GADD45γ. The GADD45 family members, GADD45α, GADD45β and GADD45γ, are identified as genotoxic stress-induced small proteins (approximately 18 kDa).[42] GADD45 family members have been

implicated in regulating a range of signaling cascades such as the MAPK cascade, DNA repair mechanism, cell cycle control and DNA demethylation.[43] The association between GADD45γ and MAPK signaling has been well established, and GADD45γ was found to be an upstream activator of the p38 MAPK and JNK pathways in many cell types (*e.g.* T cells and COS-7 cells).[44,45] Gantner *et al.* further reported that GADD45γ was a cold-inducible transcriptional activator of UCP1 and other thermogenic genes.[23] Similarly, GADD45γ$^{-/-}$ mice exhibited decreased BAT thermogenesis, hypersensitivity to cold stress and impaired oxidative capacity.[23] The mechanism underlying the role of GADD45γ was linked to adrenergic stimulation, indicating close connections with energy dissipation in brown adipocytes.[23] In this study, by performing a proteome microarray analysis, we identified GADD45γ as a target of Miltin. Specifically, Miltin treatment increased the stability of GADD45γ in both brown and white adipocytes, and the knockdown of GADD45γ antagonized the Miltin-mediated activation of thermogenesis. We further confirmed the direct interaction between Miltin and GADD45γ using biophysical methods and identified two key amino acid residues that were crucial for their binding. These results strongly support that GADD45γ is a *bona fide* target of Miltin. However, we cannot exclude that other targets are also involved in the functional regulation of Miltin.

In summary, we identified the dairy-derived peptide Miltin as a thermogenic activator in adipocytes and demonstrated its therapeutic potential for obesity and associated comorbidities. Despite the observed strengths of this study, there are certain limitations that should be addressed. First, it is possible that alterations in other tissues also contributed to the anti-obesity effect of Miltin. Second, more extended studies will focus on the function of Miltin in the prevention and treatment of T2D. Third, we cannot exclude that Miltin-mediated activation of the MAPK signaling pathways also affected other adipocyte events. However, the data presented here support further development of Miltin as a potential obesity treatment drug.

Author contributions

Hong Zhong: methodology, validation, formal analysis, investigation, data curation, writing – review & editing, funding acquisition. Xiaoxiao Zhang: methodology, validation, formal analysis, investigation, data curation. Yangyang Wu: methodology, validation, formal analysis, investigation, data curation. Lu Li: methodology, validation, investigation. Zhuo Zhang: methodology, validation, formal analysis, investigation. Xia Chi: conceptualization, validation, formal analysis, investigation, writing – review & editing, visualization, supervision. Xianwei Cui: conceptualization, writing – original draft, methodology, validation, formal analysis, investigation, data curation, supervision, funding acquisition. Chenbo Ji: conceptualization, writing – original draft, methodology, validation, formal analysis, investigation, data curation, supervision, funding acquisition.

Conflicts of interest

The authors have declared that no competing interests exist.

Acknowledgements

The work was funded by grants from the National Natural Science Foundation of China (Grant No. 81770866, 81770837, 81900783, 82070879, 82170880 and 82300949), Natural Science Foundation of Jiangsu Province (BK20190139) and 333 High-Level Talents Training Project of Jiangsu Province.

References

1 C. M. Perdomo, R. V. Cohen, P. Sumithran, K. Clement and G. Fruhbeck, Contemporary medical, device, and surgical therapies for obesity in adults, *Lancet*, 2023, **401**, 1116–1130.
2 T. D. Muller, M. Bluher, M. H. Tschop and R. D. DiMarchi, Anti-obesity drug discovery: advances and challenges, *Nat. Rev. Drug Discovery*, 2022, **21**, 201–223.
3 P. Cohen and S. Kajimura, The cellular and functional complexity of thermogenic fat, *Nat. Rev. Mol. Cell Biol.*, 2021, **22**, 393–409.
4 K. Ikeda, P. Maretich and S. Kajimura, The Common and Distinct Features of Brown and Beige Adipocytes, *Trends Endocrinol. Metab.*, 2018, **29**, 191–200.
5 M. Chondronikola, E. Volpi, E. Børsheim, C. Porter, P. Annamalai, S. Enerbäck, M. E. Lidell, M. K. Saraf, S. M. Labbe, N. M. Hurren, C. Yfanti, T. Chao, C. R. Andersen, F. Cesani, H. Hawkins and L. S. Sidossis, Brown Adipose Tissue Improves Whole-Body Glucose Homeostasis and Insulin Sensitivity in Humans, *Diabetes*, 2014, **63**, 11.
6 X. Liu, S. Wang, Y. You, M. Meng, Z. Zheng, M. Dong, *et al.*, Brown Adipose Tissue Transplantation Reverses Obesity in Ob/Ob Mice, *Endocrinology*, 2015, **156**, 2461–2469.
7 K. I. Stanford, R. J. Middelbeek, K. L. Townsend, D. An, E. B. Nygaard, K. M. Hitchcox, *et al.*, Brown adipose tissue regulates glucose homeostasis and insulin sensitivity, *J. Clin. Invest.*, 2013, **123**, 215–223.
8 F. B. Hu, J. E. Manson, M. J. Stampfer, G. Colditz, S. Liu, C. G. Solomon, *et al.*, Diet, lifestyle, and the risk of type 2 diabetes mellitus in women, *N. Engl. J. Med.*, 2001, **345**, 790–797.
9 I. A. L. Slurink, N. R. den Braver, F. Rutters, N. Kupper, T. Smeets, P. J. M. Elders, *et al.*, Dairy product consumption and incident prediabetes in Dutch middle-aged adults: the Hoorn Studies prospective cohort, *Eur. J. Nutr.*, 2022, **61**, 183–196.
10 Y. Feng, Y. Zhao, J. Liu, Z. Huang, X. Yang, P. Qin, *et al.*, Consumption of Dairy Products and the Risk of Overweight or Obesity, Hypertension, and Type 2 Diabetes Mellitus: A

Dose-Response Meta-Analysis and Systematic Review of Cohort Studies, *Adv. Nutr.*, 2022, **13**, 2165–2179.
11 N. Daniel, R. T. Nachbar, T. T. T. Tran, A. Ouellette, T. V. Varin, A. Cotillard, *et al.*, Gut microbiota and fermentation-derived branched chain hydroxy acids mediate health benefits of yogurt consumption in obese mice, *Nat. Commun.*, 2022, **13**, 1343.
12 H. Korhonen, Milk-derived bioactive peptides: From science to applications, *J. Funct. Foods*, 2009, **1**, 177–187.
13 S. Marcone, O. Belton and D. J. Fitzgerald, Milk-derived bioactive peptides and their health promoting effects: a potential role in atherosclerosis, *Br. J. Clin. Pharmacol.*, 2017, **83**, 152–162.
14 Y. Sawada, Y. Sakamoto, M. Toh, N. Ohara, Y. Hatanaka, A. Naka, *et al.*, Milk-derived peptide Val-Pro-Pro (VPP) inhibits obesity-induced adipose inflammation via an angiotensin-converting enzyme (ACE) dependent cascade, *Mol. Nutr. Food Res.*, 2015, **59**, 2502–2510.
15 S. G. Rival, C. G. Boeriu and H. J. Wichers, Caseins and casein hydrolysates. 2. Antioxidative properties and relevance to lipoxygenase inhibition, *J. Agric. Food Chem.*, 2001, **49**, 295–302.
16 L. Miclo, E. Roux, M. Genay, E. Brusseaux, C. Poirson, N. Jameh, *et al.*, Variability of hydrolysis of beta-, alphas1-, and alphas2-caseins by 10 strains of Streptococcus thermophilus and resulting bioactive peptides, *J. Agric. Food Chem.*, 2012, **60**, 554–565.
17 L. Cui, G. Yang, S. Lu, X. Zeng, J. He, Y. Guo, *et al.*, Antioxidant peptides derived from hydrolyzed milk proteins by Lactobacillus strains: A BIOPEP-UWM database-based analysis, *Food Res. Int.*, 2022, **156**, 111339.
18 C. Gomez-Gallego, I. Recio, V. Gomez-Gomez, I. Ortuno, M. J. Bernal, G. Ros, *et al.*, Effect of processing on polyamine content and bioactive peptides released after in vitro gastrointestinal digestion of infant formulas, *J. Dairy Sci.*, 2016, **99**, 924–932.
19 J. Zhu, L. Garrigues, H. Van den Toorn, B. Stahl and A. J. R. Heck, Discovery and Quantification of Nonhuman Proteins in Human Milk, *J. Proteome Res.*, 2019, **18**, 225–238.
20 X. Cui, L. You, Y. Li, L. Zhu, F. Zhang, K. Xie, *et al.*, A transcribed ultraconserved noncoding RNA, uc.417, serves as a negative regulator of brown adipose tissue thermogenesis, *Fed. Am. Soc. Exp. Biol. J.*, 2016, **30**, 4301–4312.
21 X. Cui, W. Xiao, L. You, F. Zhang, X. Cao, J. Feng, *et al.*, Age-induced oxidative stress impairs adipogenesis and thermogenesis in brown fat, *FASEB J.*, 2019, **286**, 2753–2768.
22 H. Gehart, S. Kumpf, A. Ittner and R. Ricci, MAPK signalling in cellular metabolism: stress or wellness?, *EMBO Rep.*, 2010, **11**, 834–840.
23 M. L. Gantner, B. C. Hazen, J. Conkright and A. Kralli, GADD45gamma regulates the thermogenic capacity of brown adipose tissue, *Proc. Natl. Acad. Sci. U. S. A.*, 2014, **111**, 11870–11875.
24 N. Warr, G. A. Carre, P. Siggers, J. V. Faleato, R. Brixey, M. Pope, *et al.*, Gadd45gamma and Map3k4 interactions regulate mouse testis determination via p38 MAPK-mediated control of Sry expression, *Dev. Cell*, 2012, **23**, 1020–1031.
25 M. Gao, X. Li, W. Dong, R. Jin, H. Ma, P. Yang, *et al.*, Ribosomal protein S7 regulates arsenite-induced GADD45alpha expression by attenuating MDM2-mediated GADD45alpha ubiquitination and degradation, *Nucleic Acids Res.*, 2013, **41**, 5210–5222.
26 X. Lin and H. Li, Obesity: Epidemiology, Pathophysiology, and Therapeutics, *Front. Endocrinol.*, 2021, **12**, 706978.
27 C. M. Jimenez-Munoz, M. Lopez, F. Albericio and K. Makowski, Targeting Energy Expenditure-Drugs for Obesity Treatment, *Pharmaceuticals*, 2021, **14**, 435.
28 J. L. Lau and M. K. Dunn, Therapeutic peptides: Historical perspectives, current development trends, and future directions, *Bioorg. Med. Chem.*, 2018, **26**, 2700–2707.
29 M. Muttenthaler, G. F. King, D. J. Adams and P. F. Alewood, Trends in peptide drug discovery, *Nat. Rev. Drug Discovery*, 2021, **20**, 309–325.
30 S. J. Brandt, T. D. Muller, R. D. DiMarchi, M. H. Tschop and K. Stemmer, Peptide-based multi-agonists: a new paradigm in metabolic pharmacology, *J. Intern. Med.*, 2018, **284**, 581–602.
31 C. Lee, J. Zeng, B. G. Drew, T. Sallam, A. Martin-Montalvo, J. Wan, *et al.*, The mitochondrial-derived peptide MOTS-c promotes metabolic homeostasis and reduces obesity and insulin resistance, *Cell Metab.*, 2015, **21**, 443–454.
32 Y. Li, K. Schnabl, S. M. Gabler, M. Willershauser, J. Reber, A. Karlas, *et al.*, Secretin-Activated Brown Fat Mediates Prandial Thermogenesis to Induce Satiation, *Cell*, 2018, **175**, 1561–1574.e12.
33 Z. Li, B. Zhang, N. Wang, Z. Zuo, H. Wei and F. Zhao, A novel peptide protects against diet-induced obesity by suppressing appetite and modulating the gut microbiota, *Gut*, 2023, **72**, 686–698.
34 S. Ribo, D. Sanchez-Infantes, L. Martinez-Guino, I. Garcia-Mantrana, M. Ramon-Krauel, M. Tondo, *et al.*, Increasing breast milk betaine modulates Akkermansia abundance in mammalian neonates and improves long-term metabolic health, *Sci. Transl. Med.*, 2021, **13**, eabb0322.
35 J. E. Harris, K. M. Pinckard, K. R. Wright, L. A. Baer, P. J. Arts, E. Abay, *et al.*, Exercise-induced 3′-sialyllactose in breast milk is a critical mediator to improve metabolic health and cardiac function in mouse offspring, *Nat. Metab.*, 2020, **2**, 678–687.
36 K. Nakamura, T. Kishida, A. Ejima, R. Tateyama, S. Morishita, T. Ono, *et al.*, Bovine lactoferrin promotes energy expenditure via the cAMP-PKA signaling pathway in human reprogrammed brown adipocytes, *Biometals*, 2018, **31**, 415–424.
37 F. M. Fisher, S. Kleiner, N. Douris, E. C. Fox, R. J. Mepani, F. Verdeguer, *et al.*, FGF21 regulates PGC-1alpha and browning of white adipose tissues in adaptive thermogenesis, *Genes Dev.*, 2012, **26**, 271–281.

38 E. Hondares, M. Rosell, F. J. Gonzalez, M. Giralt, R. Iglesias and F. Villarroya, Hepatic FGF21 expression is induced at birth via PPARalpha in response to milk intake and contributes to thermogenic activation of neonatal brown fat, *Cell Metab.*, 2010, **11**, 206–212.

39 D. Wolfs, M. D. Lynes, Y. H. Tseng, S. Pierce, V. Bussberg, A. Darkwah, *et al.*, Brown Fat-Activating Lipokine 12,13-diHOME in Human Milk Is Associated With Infant Adiposity, *J. Clin. Endocrinol. Metab.*, 2021, **106**, e943–e956.

40 H. Yu, S. Dilbaz, J. Cossmann, A. C. Hoang, V. Diedrich, A. Herwig, *et al.*, Breast milk alkylglycerols sustain beige adipocytes through adipose tissue macrophages, *J. Clin. Invest.*, 2019, **129**, 2485–2499.

41 M. E. Symonds, I. Bloor, S. Ojha and H. Budge, The Placenta, Maternal Diet and Adipose Tissue Development in the Newborn, *Ann. Nutr. Metab.*, 2017, **70**, 232–235.

42 G. Smaldone, D. Caruso, A. Sandomenico, E. Iaccarino, A. Foca, A. Ruggiero, *et al.*, Members of the GADD45 Protein Family Show Distinct Propensities to form Toxic Amyloid-Like Aggregates in Physiological Conditions, *Int. J. Mol. Sci.*, 2021, **22**, 10700.

43 Z. Yang, L. Song and C. Huang, Gadd45 proteins as critical signal transducers linking NF-kappaB to MAPK cascades, *Curr. Cancer Drug Targets*, 2009, **9**, 915–930.

44 B. Lu, H. Yu, C. Chow, B. Li, W. Zheng, R. J. Davis, *et al.*, GADD45gamma mediates the activation of the p38 and JNK MAP kinase pathways and cytokine production in effector TH1 cells, *Immunity*, 2001, **14**, 583–590.

45 H. Chi, B. Lu, M. Takekawa, R. J. Davis and R. A. Flavell, GADD45beta/GADD45gamma and MEKK4 comprise a genetic pathway mediating STAT4-independent IFNgamma production in T cells, *EMBO J.*, 2004, **23**, 1576–1586.